Journal of Renewable Materials

Tech Science Press

https://doi.org/10.32604/jrm.2026.02026-0043

ARTICLE

Design and Functional Characterisation of Bio-Based Multilayer Polylactic Acid Films Incorporating Chitosan and Propolis for Antimicrobial Food Packaging Applications

Ahmad Bustaman N. A. H.[1], **Han Lyn Foong**[2], **Stefan Schiessl**[3] **and Nur Hanani Z. A.**[1,4,*]

[1]Department of Food Technology, Faculty of Food Science and Technology, Universiti Putra Malaysia, UPM Serdang, Selangor, Malaysia

[2]Department of Diagnostic & Allied Health Science, Faculty of Health and Life Sciences, Management and Science University, No. 4, Persiaran Olahraga, Section 13, Shah Alam, Selangor Darul Ehsan, Malaysia

[3]Fraunhofer Institute for Process Engineering and Packaging IVV, Freising, Germany

[4]Institute of Nanoscience and Nanotechnology, Universiti Putra Malaysia, UPM, Serdang, Selangor, Malaysia

*Corresponding Author: Nur Hanani Z. A. Email: hanani@upm.edu.my

Received: 25 March 2026; Accepted: 07 September 2026; Published: 27 October 2026

ABSTRACT: The development of renewable and bio-based materials with functional performance comparable to conventional plastics remains a key challenge in sustainable packaging. In this study, bio-based multilayer films were fabricated using polylactic acid (PLA) as a renewable polyester substrate, combined with chitosan (CS) and propolis (PRP) as naturally derived functional layers. Sequential surface coating enabled the formation of multilayer architectures integrating complementary structural and antimicrobial properties from bio-derived constituents. Trilayer PLA/CS/PRP films exhibited significantly increased thickness and opacity compared with neat PLA, along with higher ($p < 0.05$) water vapour permeability. Mechanical analysis showed significant reductions ($p < 0.05$) in tensile strength and elongation at break, reflecting interfacial and structural effects associated with multilayer integration. The preservation performance of the multilayer films was evaluated using fresh mozzarella cheese stored at 4°C for 25 days. Compared with neat PLA, the multilayer films more effectively suppressed the growth of total aerobic bacteria, yeast, and mould during refrigerated storage of mozzarella cheese. Although direct antimicrobial activity of the films was not evaluated, the multilayer system demonstrated improved preservation performance by maintaining pH stability, reducing weight loss, and delaying microbial proliferation. These findings suggest the potential of multilayer bio-based coating strategies for active packaging applications in perishable food products.

KEYWORDS: Active packaging; antimicrobial; biodegradable; water vapour permeability; opacity

1 Introduction

Growing environmental concerns and regulatory pressures to reduce plastic waste have intensified interest in sustainable food packaging materials. Despite the rapid growth of bio-based plastic from 1.6 to 3.0 million tonnes between 2021 and 2023, conventional petrochemical plastics still dominate global production, exceeding 400 million tonnes annually [1,2]. Among biodegradable polymers, polylactic acid (PLA) has emerged as one of the most commercially viable alternatives due to its renewability, compostability, processability, and regulatory acceptance for food-contact applications. Nevertheless, the broader application of PLA in food packaging remains constrained by its moderate moisture barrier performance, relatively high

Copyright © 2026 The Authors. Published by Tech Science Press. This work is licensed under a Creative Commons Attribution 4.0 International License, which permits unrestricted use, distribution, and reproduction in any medium, provided the original work is properly cited.

gas permeability, brittleness, and lack of inherent antimicrobial functionality [3,4]. These limitations are particularly critical for packaging high-moisture, microbiologically sensitive foods.

To overcome these limitations, composite and multilayer film systems have been increasingly explored. Multilayer designs enable the strategic combination of materials with complementary properties, allowing mechanical integrity, barrier performance, and active functionality to be optimised simultaneously [5]. In this context, the incorporation of antimicrobial agents into biodegradable polymer matrices has gained considerable attention as a means of extending food shelf life while reducing reliance on synthetic preservatives. A wide range of natural and synthetic antimicrobials have been investigated for this purpose, including essential oils [6–8], plant extracts [9–11], and metal oxides [12,13]. Previous studies have demonstrated that even low loadings of antimicrobial compounds can substantially enhance packaging performance. For example, Zehetmeyer et al. [14] reported a two-order-of-magnitude increase in antimicrobial activity in PBAT films containing only 0.5 wt% nisin.

Propolis (PRP), a resinous substance produced by honeybees from plant exudates, has attracted growing interest as a natural antimicrobial agent for food preservation. [15–17]. In previous studies, PRP solution at a concentration of 10% has been reported to inhibit spoilage bacteria and fungi commonly associated with cheese, while exerting comparatively limited effects on lactic acid bacteria (LAB), which are essential for flavour and texture development in fermented dairy products [17,18]. Additionally, alcohol-soluble PRP fractions have been demonstrated to exhibit stronger antibacterial effects against Gram-positive than Gram-negative bacteria [19,20]. However, direct incorporation of PRP into packaging materials can present challenges, including intense colouration, strong odour, and potential sensory impacts at higher concentrations [21]. These drawbacks highlight the need for controlled-release strategies and synergistic formulations that allow antimicrobial efficacy at reduced PRP loadings.

Chitosan (CS), a partially deacetylated derivative of chitin, is another promising biopolymer for active packaging applications. CS is biodegradable, biocompatible, and exhibits intrinsic antimicrobial activity against a broad spectrum of bacteria and fungi, primarily through electrostatic interactions with microbial cell membranes [22–24]. Moreover, CS is compatible with PLA in multilayer configurations and can function as both an antimicrobial agent and a functional interlayer, potentially modulating the release of incorporated active compounds. Synergistic antimicrobial effects between CS and PRP have been reported in edible coatings and films, suggesting enhanced efficacy when these agents are combined [25]. Both CS and PRP are classified as Generally Recognised as Safe (GRAS) and are approved for food-related applications in multiple jurisdictions [26,27].

Fresh mozzarella cheese represents a particularly challenging food matrix for packaging innovation. Characterised by high moisture content (~60%), mild acidity (pH ≈ 5.7), and limited salt concentration, fresh mozzarella is highly susceptible to microbial spoilage and quality deterioration during refrigerated storage [28,29]. Its shelf life typically ranges from only a few days for artisanal products to approximately 20 days for industrially packaged variants [30]. Spoilage is primarily driven by the growth of non-lactic acid bacteria, psychrotrophic microorganisms, yeasts, and moulds, which negatively affect texture, flavour, and safety [29]. Effective packaging solutions must therefore balance moisture control, gas permeability, and antimicrobial protection without compromising product quality.

Although PRP has been incorporated into various biopolymeric matrices, including PLA [31], CS [32], starch [33], and petrochemical-based plastics [34], studies investigating sequentially coated PLA/CS/PRP multilayer films for preserving fresh mozzarella cheese remain limited. Therefore, this study aimed to evaluate the physicochemical properties and preservation performance of this multilayer system for maintaining storage quality of fresh mozzarella cheese. This study aligns with the United Nations Sustainable Development Goals (SDGs), particularly SDG 12: Responsible Consumption and Production.

2 Materials and Methods

2.1 Materials

PLA films (NATIVA®) were supplied by Taghleef Industries (Holzhausen an der Haide, Germany) to the Fraunhofer Institute, IVV. Raw buffalo milk was obtained from a local dairy supplier (Barkath Fresh, Ampang, Malaysia). Rennet was obtained from Chr. Hansen (Hoersholm, Denmark). Propolis extract from *Apis mellifera* L. was purchased from Take It Global (Kuala Lumpur, Malaysia), while CS was obtained from Maple Lifescience (Gyeonggi-do, Korea). Acetic acid (1% v/v), citric acid, sodium chloride, and glutaraldehyde were supplied by Systerm (Shah Alam, Malaysia). Microbiological media included plate count agar (PCA), de Man, Rogosa and Sharpe agar (Oxoid Ltd., Cheshire, England), and potato dextrose agar (PDA) (Merck, Darmstadt, Germany). All chemicals were of analytical grade and used as received unless otherwise stated.

2.2 Film Preparation

Multilayer film samples were prepared by sequential surface coating following the approach of Karpuz and Palabiyik [18] with modifications. For the PRP layer, a 10% (w/v) solution was prepared by dissolving 10 g of propolis extract in 100 mL of ethyl acetate. This concentration was selected based on preliminary trials, as higher PRP concentrations resulted in excessive surface stickiness after drying. The mixture was agitated at 150 rpm for 6 h at room temperature (25 ± 2°C) using a shaker incubator (Infors HT Ecotron, Switzerland). A fixed volume (10 mL) of the PRP solution was applied uniformly onto PLA films (28 cm × 40 cm) using a wire bar coater (wet film thickness: 100 µm; film width: 32 cm; ChemInstruments, Fairfield, USA). However, dry coating mass, coating yield, residual solvent content, residual glutaraldehyde, coating uniformity, and individual layer thicknesses were not quantified in the present study. The coated films were air-dried at ambient conditions for 6 h to allow solvent evaporation.

For the CS layer, a 0.1% (w/v) solution was prepared in 1% (v/v) acetic acid and stirred for 20 min until fully solubilised. A volume of 10 mL was applied onto PLA films using the same wire-bar coating technique. To induce crosslinking of the CS layer, 3 mL of 0.5% (v/v) glutaraldehyde solution was uniformly sprayed onto the coated film surface. The selected glutaraldehyde concentration was based on preliminary trials to achieve adequate coating stability while minimising excessive film brittleness. The coated films were subsequently dried using a hot-air dryer at 65 ± 15°C for 10 min to facilitate crosslinking and solvent evaporation. Surface temperature was continuously monitored using an infrared thermometer (Fluke, Everett, USA) to maintain the desired temperature range and minimise localised overheating or hotspot formation during drying.

For trilayer PLA/CS/PRP films, the PRP layer was applied only after CS-coated films had been dried at 65 ± 15°C for 10 min under the standardised drying conditions described above. Residual moisture content of the CS layer was not directly measured and should therefore be considered a limitation of the present study. Preliminary observations suggested that this coating sequence resulted in improved coating integrity, whereas the reverse coating order (PRP/CS) showed signs of partial layer separation. A schematic representation of the multi-layer films is presented in Fig. 1. All films were conditioned at 25 ± 2°C and 50 ± 2% relative humidity (RH) for at least 48 h prior to analyses.

2.3 Thickness

Film thickness was measured with a digital micrometer (Mitutoyo Co., Kawasaki-Shi, Japan) with 0.1 µm resolution. Measurements were taken at five random positions per film, and results were expressed as mean ± standard deviation.

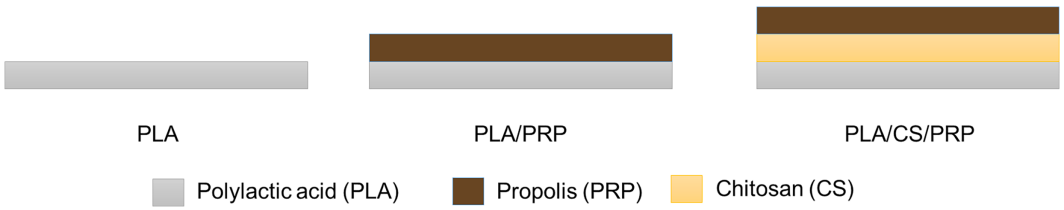

Figure 1: Illustration of the cross-sections of the polylactic acid (PLA), polylactic acid/propolis (PLA/PRP), and polylactic acid/chitosan/propolis (PLA/CS/PRP) films. Images are not to scale.

2.4 Mechanical Strength

Tensile strength (TS), Young's modulus (YM), and elongation at break (EAB) of the films were determined according to ASTM D882 [35], following the procedure described by Ordoñez et al. [36]. Film specimens were cut into strips (1.5 cm × 9 cm) and mounted on a universal testing machine (Instron 3366, Canton, USA) with an initial separation of 50 mm. Tests were conducted at a crosshead speed of 5 mm min^{-1} under ambient conditions.

2.5 Optical Properties

Film colour was evaluated in the CIELAB colour space [17] using a calibrated colourimeter (WR-10, FRU, Shenzhen, China). Results were expressed as L^* (lightness), a^* (red-green), and b^* (yellow-blue) values.

Opacity and transparency were evaluated using a UV-VIS spectrophotometer (Ruili Analytical Instrument Co., Beijing, China) [37] and calculated using the formula below:

$$\text{Opacity } \left(\text{AU mm}^{-1}\right) = \frac{A_{600}}{x} \tag{1}$$

$$\text{Transparency} = \frac{-\log T_{600}}{x} \tag{2}$$

where A_{600} and T_{600} represent light absorbance (AU) and percent transmittance (%) at 600 nm, respectively, and x is film thickness (mm).

2.6 Moisture Content and Water Solubility

Moisture content was determined following ASTM D644-99 [38]. Film strips (6 cm × 1 cm) were weighed, oven-dried at 110°C for 24 h. Then, the samples were weighed immediately at ambient conditions (25 ± 2°C, 50 ± 5% RH). Moisture content was calculated as:

$$\text{Moisture content } (\%) = \left(\frac{w_0 - w_1}{w_1}\right) \times 100 \tag{3}$$

Water solubility was determined by immersing dried film strips in distilled water for 24 h. The insoluble fraction was re-dried at 130°C for 24 h and weighed. Water solubility was calculated as:

$$\text{Water solubility } (\%) = \left(\frac{w_1 - w_2}{w_1}\right) \times 100 \tag{4}$$

where w_0 is initial weight (g), w_1 is the oven-dried weight (g), and w_2 is the final oven-dried weight of the insoluble fraction (g).

2.7 Water Vapour Permeability (WVP)

WVP was determined gravimetrically according to ASTM E96 method [39] with modifications. Film samples were sealed over permeation cups containing 6 mL distilled water. The permeation cups were sealed using silicone grease to minimise edge leakage. The cups were subsequently placed in a desiccator containing anhydrous silica gel (previously regenerated at 120°C for 3 h), which maintained the external relative humidity at approximately 0%–5% RH. This produced a water vapour pressure gradient of approximately 100% RH (inside cup, 25°C) to ~0% RH (outside), equivalent to a driving pressure difference (P) of approximately 3168.74 Pa. Weight loss was recorded hourly for 8 h period, and steady-state permeation behaviour was confirmed by linear regression of mass loss vs. time ($R^2 > 0.99$) prior to calculation (Fig. S1). WVP was calculated as:

$$\text{WVP}\ \left(\text{g m}^{-1}\,\text{s}^{-1}\,\text{Pa}^{-1}\right) = \frac{\Delta w \cdot l}{A \cdot t \cdot P} \tag{5}$$

where Δw is the weight loss (g), l is the film thickness (m), A is the exposed area (0.0028 m^2), t is time (s), and P is the water vapour pressure difference at 25°C (3168.74 Pa) which approximates the effective driving pressure difference under the ~100% to ~0% RH gradient established by the anhydrous silica gel desiccator. It is acknowledged that this near-zero external RH condition is considerably drier than conditions encountered in typical food packaging applications and therefore, is noted as a limitation when interpreting absolute WVP values in comparative contexts.

2.8 Fourier Transform Infrared (FTIR) Spectroscopy

FTIR spectra were recorded using a SHIMADZU FTIR-8400S spectrometer (Shimadzu Corporation, Kyoto, Japan) equipped with an attenuated total reflectance (ATR) accessory. Spectra were acquired at room temperature (25 ± 2°C) over the wavenumber range of 500–3250 cm^{-1} with a spectral resolution of 4 cm^{-1}. Each spectrum was obtained from 16 accumulated scans to improve the signal-to-noise ratio. A background spectrum was obtained using a blank cell prior to measurements. All spectra were analysed using the integrated LabSolutions IR software (Shimadzu Corporation, Kyoto, Japan).

2.9 Mozzarella Cheese Preparation and Storage Study

Raw buffalo milk (1.5 L) was heated over low heat with constant stirring. At 31.5°C, citric acid (3.24% w/v) was added, followed by rennet (1.21% w/v) at 32°C. The mixture was left for 5 min to form curds, which were then cut and gently stirred while heating to 40°C. Whey was separated using sterile muslin cloth, and the curds were immersed in salted whey (23 g NaCl) at 85°C and manually stretched until a smooth, elastic, and fibrous mozzarella texture was obtained. The prepared mozzarella cheese was cut into blocks (4.5 cm × 5 cm), with three independent cheese samples prepared for each packaging treatment. The knives and cutting boards were sanitised using sodium hypochlorite solution (200 ppm) and rinsed with sterile distilled water prior to use. Samples were individually wrapped using PLA, PLA/PRP, or PLA/CS/PRP films (7.5 cm × 9 cm) under atmospheric packaging conditions (25 ± 2°C, 50 ± 5% RH) and stored at 4 ± 1°C for 25 days. Physicochemical and microbiological analyses were performed at 5-day intervals (days 0, 5, 10, 15, 20, and 25).

2.10 Characterization of Mozzarella Cheese

2.10.1 Weight Loss

Weight loss was determined by comparing the initial weight of the fresh cheese sample with weight after storage:

$$\text{Weight loss}\ (\%) = \frac{w_0 - w_1}{w_0} \times 100 \tag{6}$$

where w_0 is the sample weight (g) at day 0 and w_1 is the sample weight (g) after storage.

2.10.2 Colour and pH

Colour of cheese samples along the storage period was measured using a calibrated colourimeter (WR-10, FRU Instruments, Shenzhen City, China). To determine pH, 10 g of cheese was weighed and homogenised with 90 mL of distilled water for 2 min at room temperature. The pH of the slurry was then measured using a calibrated digital pH meter (pH 700, Eutech Instruments Pte Ltd., Singapore).

2.10.3 Microbiological Analysis

Microbiological counts were performed according to methods of Huang et al. [30] with slight modifications. Ten grams of cheese were homogenized in 90 mL sterile 0.9% NaCl solution using a stomacher for 2 min. Ten-fold serial dilutions were prepared, and 0.1 mL of the appropriate dilution was plated on:

- PCA for total viable count (TVC), incubated at 30 ± 1°C for 48 h,
- MRS agar for lactic acid bacteria, incubated at 37 ± 1°C for 48 h,
- PDA for yeast and moulds, incubated at 25 ± 1°C for 48 h.

Results were expressed as log CFU/g. Microbiological analyses were performed in triplicate using three independently packaged cheese samples for each treatment and storage interval.

2.11 Statistical Analysis

All experiments were performed in triplicate. Data were analysed using one-way analysis of variance (ANOVA) followed by Tukey's post hoc test (SPSS v25.0). Statistical significance was set at $p < 0.05$.

3 Results and Discussion

3.1 Thickness and Optical Properties

Film thickness is a critical structural parameter in polymeric materials, as it directly influences barrier properties, mechanical behaviour, and overall material performance. As shown in Table 1, the deposition of the PRP layer resulted in a significant increase ($p < 0.05$) in thickness from 27 to 45 μm. This increase is attributed to the formation of a continuous coating layer on the PLA substrate, contributing additional mass and structural heterogeneity. A similar trend has been reported by Roy et al. [40], where incorporation of PRP into CS-based films increased thickness approximately 25%.

Subsequent incorporation of the CS layer further increased ($p < 0.05$) the thickness to 57 μm. This behaviour can be associated with the formation of a secondary polymeric network at the PLA interface, where CS chains establish a coherent layer through intermolecular interactions and crosslinking.

Table 1: Film thickness, opacity, and transparency of polylactic acid (PLA), polylactic acid/propolis (PLA/PRP), and polylactic acid/chitosan/propolis (PLA/CS/PRP) films.

Film	Thickness (μm)	Opacity (AU mm^{-1})	Transparency
PLA	27.06 ± 0.25^{c}	3.51 ± 0.36^{b}	3.49 ± 0.01^{b}
PLA/PRP	45.12 ± 0.11^{b}	40.37 ± 20.43^{a}	0.51 ± 0.04^{a}
PLA/CS/PRP	57.02 ± 0.11^{a}	45.92 ± 8.33^{a}	0.91 ± 0.07^{a}

Note: Values are given as mean ± SD (n = 3). Means in the same column that do not share a letter are significantly different ($p < 0.05$).

From an optical perspective, neat PLA films exhibited high transparency, reflecting their relatively homogeneous and amorphous structure. However, the introduction of PRP and CS layers significantly increased ($p < 0.05$) opacity and reduced transparency. This effect can be attributed to increased light scattering arising from refractive index mismatches between the PLA substrate and the coated layers, as well as the presence of dispersed PRP constituents. In particular, PRP contains waxes and resinous compounds, which may account for its intrinsic turbidity and contribute to microstructural heterogeneities within the coating [41]. Similar increases in opacity with PRP incorporation have been reported biopolymer-based films [42].

The incorporation of PRP also significantly ($p < 0.05$) altered the colour attributes (L^*, a^*, b^*) of the films (Table 2). The lower L^* value indicates a dark, almost black appearance consistent with the deep brown colouration characteristic of PRP extract. The increase in b^* values reflect a noticeable shift towards yellowness attributable to the presence of flavonoids naturally present in PRP [43], and comparable trends have been reported in biopolymer films incorporating ethanolic PRP extracts [37,44,45].

Table 2: Total colour difference and CIE L^* a^* b^* colour coordinates of polylactic acid (PLA), polylactic acid/propolis (PLA/PRP), and polylactic acid/chitosan/propolis (PLA/CS/PRP) films.

Film	Total Colour Difference (ΔE)	L^*	a^*	b^*
PLA	0.00 ± 0.00^{b}	56.02 ± 0.00^{a}	1.05 ± 0.33^{b}	-0.55 ± 0.00^{b}
PLA/PRP	20.27 ± 20.28^{a}	1.05 ± 0.33^{b}	0.34 ± 0.00^{a}	6.27 ± 1.10^{a}
PLA/CS/PRP	19.26 ± 1.03^{a}	1.23 ± 0.33^{b}	1.23 ± 0.19^{a}	5.48 ± 3.20^{a}

Note: Values are given as mean ± SD (n = 3). Means in the same column that do not share a letter are significantly different ($p < 0.05$).

In contrast, the incorporation of the CS layer did not significantly affect the L^*, a^*, or b^* values ($p \geq 0.05$). This can be attributed to the inherently low chromaticity of CS and its relatively low concentration in the multilayer structure [46]. Furthermore, its intermediate positioning within the multilayer configuration may limit its direct contribution to surface optical properties. Overall, the observed optical changes highlight the influence of bio-based functional layers on light transmission behaviour, which is an important consideration in the design of renewable polymer materials for packaging applications.

3.2 Moisture Content, Water Solubility, and Water Vapour Permeability (WVP)

Moisture content, water solubility, and water vapour permeability (WVP) are key parameters governing the performance of bio-based polymer films, particularly in applications involving high-moisture food systems. As summarised in Table 3, neat PLA film exhibited a low moisture content of 1.24%, reflecting the relatively hydrophobic nature and low polarity of the polyester backbone. Upon deposition of the PRP

layer, moisture content decreased significantly ($p < 0.05$) to 0.06%. This reduction can be attributed to the hydrophobic character of PRP, which limits the availability of polar sorption sites for water molecules. In addition, the use of ethyl acetate as a solvent may induce transient surface restructuring during evaporation, resulting in reduced surface affinity towards moisture [47]. The formation of a dense PRP coating layer may also increase diffusion path tortuosity, thereby restricting moisture uptake, although further structural characterisation using SEM or contact angle analysis is required to confirm this mechanism. Comparable reductions in moisture content have been reported for polymeric systems modified with hydrophobic surface coatings [48,49].

Table 3: Moisture content, water solubility, and water vapour permeability (WVP) of polylactic acid (PLA), polylactic acid/propolis (PLA/PRP), and polylactic acid/chitosan/propolis (PLA/CS/PRP) films.

Film	Moisture Content (%)	Water Solubility (%)	WVP ($\times 10^{-8}$ g m^{-1} s^{-1} Pa^{-1})
PLA	1.24 ± 0.11^{b}	1.21 ± 0.23^{a}	1.38 ± 0.10^{b}
PLA/PRP	0.06 ± 0.05^{c}	0.16 ± 0.08^{b}	3.60 ± 0.53^{a}
PLA/CS/PRP	2.18 ± 0.19^{a}	1.78 ± 0.14^{a}	2.63 ± 0.24^{a}

Note: Values are given as mean ± SD (n = 3). Means in the same column that do not share a letter are significantly different ($p < 0.05$).

In contrast, the incorporation of the CS layer led to a significant increase ($p < 0.05$) in moisture content to 2.18%, corresponding to approximately 1.8-fold and 36-fold increases relative to neat PLA and PLA/PRP films, respectively. This behaviour is consistent with the hydrophilic nature of CS, which contains abundant amino and hydroxyl functional groups capable of forming hydrogen bonds with water molecules [50–52].

Water solubility provides insight into the stability of polymer films under aqueous conditions. Neat PLA film exhibited low solubility (1.21%), which further decreased to 0.16% following PRP coating. This reduction is associated with the predominantly hydrophobic composition of PRP, consisting of polyphenolic resins, waxes, and fatty acids with limited polar functionality [53,54]. The presence of these components likely reduces polymer–water interactions and inhibits matrix disintegration. The reduction in water solubility further contributes to the preservation of film structural integrity, particularly under refrigerated storage conditions, where chilled packaging systems are susceptible to condensation-induced moisture exposure.

Conversely, the addition of the CS layer significantly increased solubility ($p < 0.05$), reflecting the water affinity of its functional groups and its partial solubilisation in aqueous environments [51,55].

WVP is a critical transport parameter that determines the ability of packaging materials to regulate moisture migration. Interestingly, the incorporation of PRP significantly increased ($p < 0.05$) WVP from 1.38 to 3.60 $\times 10^{-8}$ g m^{-1} s^{-1} Pa^{-1} relative to neat PLA, despite the reduction in moisture content. This apparent inconsistency may be attributed to partial solvent-induced surface modification or plasticisation of the PLA matrix by ethyl acetate present in the PRP solution. Such interactions can induce microstructural defects, including microcracks or increased surface roughness, which facilitate vapour diffusion pathways and enhance water transport [56]. Comparable propolis-related changes in water-vapour barrier behaviour have been reported for PLA-based systems [37,57], where hydrophilic/hydrophobic imbalance and surface-defect formation from propolis incorporation were similarly implicated in altered vapour transport.

The subsequent addition of the CS layer significantly reduced ($p < 0.05$) WVP relative to PLA/PRP films. This improvement is likely attributed to the formation of a more compact and continuous multilayer architecture, which may increase the tortuosity of diffusion pathways and reduce the effective free volume available for water vapour migration, although cross-sectional SEM analysis is required to verify this

structural interpretation. Nevertheless, the WVP of PLA/CS/PRP remained higher than that of neat PLA, indicating that the inherent hydrophilicity of CS partially offsets the barrier enhancement by promoting water sorption and facilitating limited molecular transport within the biopolymeric phase. These findings are consistent with Garavand et al. [22], who reported limited changes in WVP in PLA systems modified with CS.

3.3 Mechanical Properties

Young's modulus (YM), tensile strength (TS), and elongation at break (EAB) are presented in Table 4. Neat PLA film exhibited the highest ($p < 0.05$) YM value (2.93 GPa), consistent with the reported range of 2.0–3.5 GPa for PLA [58,59], reflecting the relatively rigid nature of the polyester backbone and limited chain mobility. The incorporation of PRP and CS layers resulted in a significant decrease ($p < 0.05$) in YM, indicating reduced stiffness of the multilayer system, which can be attributed to the introduction of less rigid, heterogeneous surface layers and disruption of stress transfer across the film thickness.

Table 4: Young's modulus (YM), elongation at break (EAB), and tensile strength (TS) of polylactic acid (PLA), polylactic acid/propolis (PLA/PRP), and polylactic acid/chitosan/propolis (PLA/CS/PRP) films.

Film	YM (GPa)	EAB (%)	TS (MPa)
PLA	2.93 ± 0.19^{a}	16.49 ± 5.08^{a}	39.70 ± 4.41^{a}
PLA/PRP	1.15 ± 0.15^{b}	4.55 ± 2.22^{b}	21.04 ± 3.39^{b}
PLA/CS/PRP	0.73 ± 0.06^{c}	3.25 ± 0.49^{b}	14.81 ± 4.19^{b}

Note: Values are given as mean ± SD (n = 3). Means in the same column that do not share a letter are significantly different ($p < 0.05$).

This trend contrasts with the findings of Kamaludin et al. [60], who reported an increase in YM following CS incorporation into PLA via melt-compounding, attributable to the microphase separation and reduced chain mobility. The discrepancy is likely related to differences in processing methods and resulting microstructures. In melt-compounding systems, CS may be more uniformly distributed within the PLA matrix, promoting microphase interactions and restricting chain mobility. In contrast, the sequential assembly method employed in this study generates discrete layered interfaces, where limited interdiffusion between PLA and CS phases may reduce interfacial adhesion and load transfer efficiency.

Neat PLA films also exhibited the highest ($p < 0.05$) TS (39.70 MPa) and EAB (16.49%), values comparable to conventional petrochemical-based polymers such as low-density polyethylene (10–45 MPa) [61] and polypropylene (30–40 MPa) [62,63]. The reduction in TS and EAB following PRP and CS deposition suggests that multilayer formation introduces structural discontinuities and weak interfacial regions. In particular, poor interfacial compatibility between the hydrophobic PLA substrate and hydrophilic CS layer may result in stress concentration sites and premature failure under tensile loading [60,64]. Additionally, exposure to ethyl acetate during PRP deposition may induce surface plasticisation or partial degradation of PLA, further compromising mechanical integrity. The deterioration in mechanical properties may partially support the proposed presence of microstructural defects or interfacial discontinuities within the multilayer system, corroborating the higher WVP observed after PRP incorporation.

Although glutaraldehyde crosslinking of CS is generally reported to enhance water resistance and mechanical strength [65,66], excessive or spatially confined crosslinking at the surface may lead to the formation of brittle, highly crosslinked domains with limited capacity for energy dissipation [67]. Such localised rigidity can reduce overall film flexibility and contribute to reduced EAB. Optimisation of

crosslinking conditions, including reducing glutaraldehyde concentration or promoting more homogeneous distribution within the CS layer, may improve interfacial cohesion and mechanical performance.

3.4 Fourier Transform Infrared (FTIR) Spectroscopy

FTIR spectroscopy was employed to elucidate intermolecular interactions among PLA, CS, and PRP constituents within the multilayer structure (Fig. 2). Neat PLA films exhibited characteristic absorption bands at 2995 and 2946 cm^{-1} (C-H stretching), 1748 cm^{-1} (C=O stretching), and 1181 cm^{-1} (C-O-C stretching), consistent with the ester functional groups of the PLA backbone [68–70].

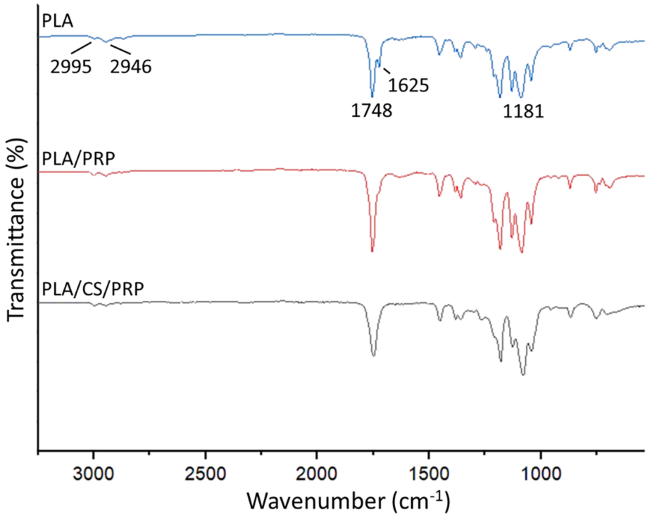

Figure 2: FTIR spectra for polylactic acid (PLA), polylactic acid/propolis (PLA/PRP), and polylactic acid/chitosan/propolis (PLA/CS/PRP) films.

In PLA/PRP film, the slight shift of the C=O stretching peak to 1756 cm^{-1} was observed, which may suggest weak intermolecular interactions between PLA and PRP components. It should be noted that classical hydrogen bonding, in which a phenolic hydroxyl group acts as a proton donor to the PLA carbonyl oxygen, would be expected to weaken the C=O bond and shift its stretching frequency to a lower wavenumber. Therefore, the observed high-wavenumber shift is more consistent with weaker, non-specific dipole-dipole interactions between the polar PLA ester carbonyl and the phenolic/flavonoid moieties of PRP, which can restrict local carbonyl segmental mobility without full proton transfer to the carbonyl oxygen [71]. A comparable phenomenon has been reported for PLA/chitosan-based films, where new hydrogen bonding introduced by an incorporated flavonoid was instead reflected as a lower-wavenumber shift of the hydroxyl-related band rather than the carbonyl band, indicating that the carbonyl region alone does not selectively track hydrogen-bond formation in these systems [72].

Additional spectral features in the 1200–1000 cm^{-1} region can be attributed to overlapping C-O and O-H vibrations of phenolic compounds, while increased intensity near 1456 cm^{-1} may be associated with aromatic ring vibrations from flavonoid constituents [73].

The incorporation of the CS layer resulted in relatively minor changes in the overall FTIR spectrum, likely due to its intermediate position within the multilayer architecture and limited surface exposure. However, the appearance of a broader and more pronounced band in the 1020–1070 cm^{-1} region can be attributed to C-O stretching vibrations of the polysaccharide backbone, confirming the presence of CS within the multilayer system.

Notably, the peak at 1625 cm^{-1}, observed in the PLA and PLA/PRP films, is plausibly attributed to aromatic C=C stretching vibrations of the phenolic and flavonoid constituents of PRP, possibly overlapping with the H-O-H bending mode of residual absorbed water (~1640 cm^{-1}). Comparable absorption bands in the 1600–1635 cm^{-1} region have been reported for CS-PRP and other PRP-enriched biopolymer films and attributed to aromatic ring C=C stretching and N-H bending vibrations associated with flavonoid and phenolic acid constituents of propolis [74,75]. The persistence and slight intensification of this band across the PLA/PRP and PLA/CS/PRP films may therefore reflect changes in the local hydration state and the aromatic-ring environment of PRP-associated phenolics, consistent with the occurrence of intermolecular interactions among PLA, CS, and PRP components.

3.5 Colour of Mozzarella Cheese

Colour stability during storage reflects the ability of packaging materials to regulate environmental exposure, including moisture loss, oxygen ingress, and light transmittance. Cheese packaged in neat PLA film exhibited a progressive decrease in L^* (Fig. 3a) and a^* values (Fig. 3b) as well as an increase in b^* values (Fig. 3c) after day 15, indicating surface yellowing likely associated with dehydration (Fig. 4) [76]. Fluctuations in b^* values may also be linked to the degradation of photosensitisers such as riboflavin and carotenoids during lipid oxidation [77,78]. Importantly, incorporation of PRP, with or without the CS layer, did not result in significant colour transfer to the cheese, suggesting limited migration of PRP pigments under the conditions tested. These findings are consistent with previous studies reporting minimal sensory impact of PRP-containing films on dairy products [21] and address concerns regarding pigment migration from propolis extract [45].

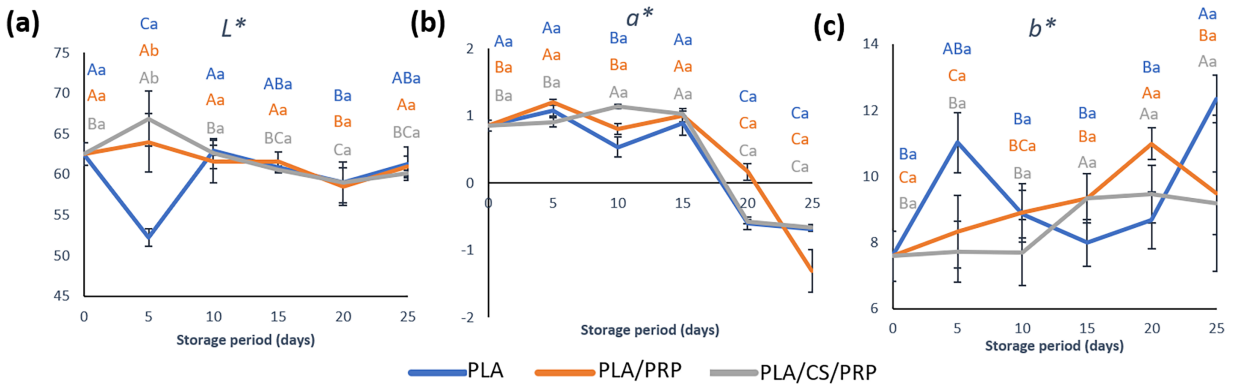

Figure 3: Colour change, represented by the (**a**) L^*, (**b**) a^*, and (**c**) b^* indices of mozzarella cheese packaged in polylactic acid (PLA), polylactic acid/propolis (PLA/PRP), and polylactic acid/chitosan/propolis (PLA/CS/PRP) films during 25 days of storage at 4°C. Values are presented as mean ± SD (n = 3). Different lowercase letters indicate significant differences among packaging treatments at the same storage day ($p < 0.05$) while different uppercase letters indicate significant differences among storage days for the same packaging treatment.

3.6 pH and Weight Loss of Mozzarella

The evolution of pH during storage (Fig. 5a) reflects microbial activity and biochemical changes within the cheese matrix. The initial pH (5.87) was slightly higher than the typical range for fresh mozzarella (5.5 to 5.7) [79], likely reflecting variability in milk composition, mineral content, or processing conditions [80]. The gradual decrease in pH across all samples is consistent with ongoing microbial metabolism. Notably, cheese packaged in PLA/CS/PRP films exhibited the smallest pH decline ($p < 0.05$), suggesting

delayed acidification. This behaviour may suggest a potential role of the CS layer in modulating compound diffusion [81]; however, release kinetics were not measured and this remains speculative.

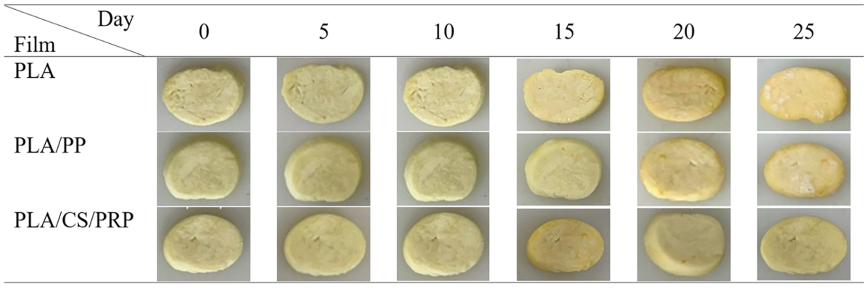

Figure 4: Appearance of mozzarella cheese packaged in polylactic acid (PLA), polylactic acid/propolis (PLA/PRP), and polylactic acid/chitosan/propolis (PLA/CS/PRP) films during 25 days of storage at 4°C.

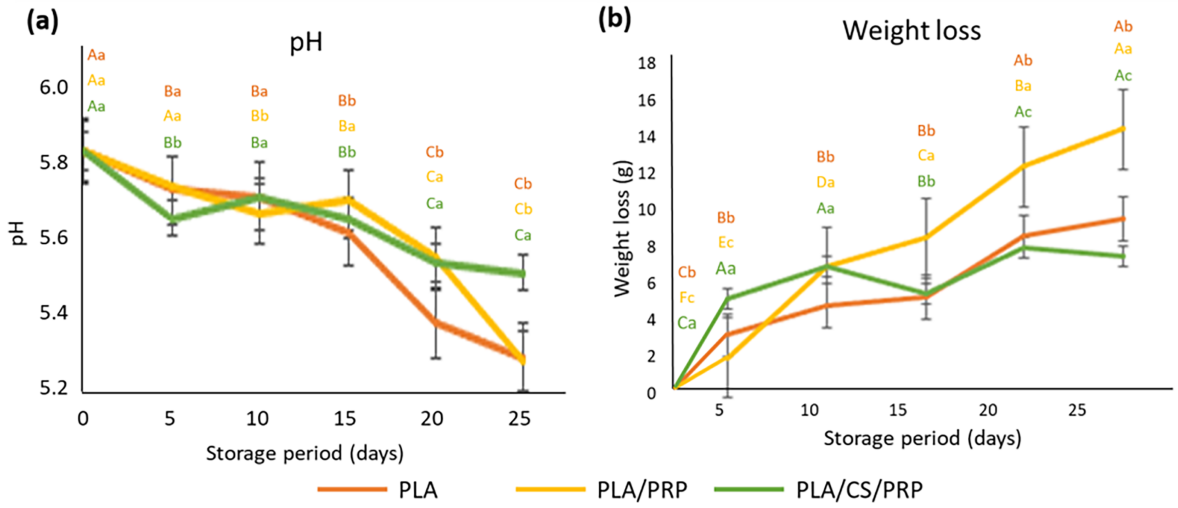

Figure 5: (**a**) pH change and (**b**) weight loss of mozzarella cheese packaged in polylactic acid (PLA), polylactic acid/propolis (PLA/PRP), and polylactic acid/chitosan/propolis (PLA/CS/PRP) films during 25 days of storage at 4°C. Values are presented as mean ± SD (n = 3). Different lowercase letters indicate significant differences among packaging treatments at the same storage day ($p < 0.05$) while different uppercase letters indicate significant differences among storage days for the same packaging treatment.

Weight loss trends (Fig. 5b) further reflect the moisture barrier performance of the films. The highest weight loss ($p < 0.05$) observed in PLA/PRP film is consistent with their elevated WVP. In contrast, PLA/CS/PRP films exhibited an initial increase in weight loss followed by stabilisation, which may be attributed to moisture absorption and swelling of the CS layer. This swelling can potentially reduce free volume and fill microvoids within the structure, forming a more effective secondary barrier over time [82]. Nevertheless, detailed structural analyses are necessary to confirm this.

3.7 Microbial Analysis

The microbial stability of fresh mozzarella cheese is strongly influenced by packaging material properties, particularly barrier performance and the presence of antimicrobial functionalities. The initial total viable counts (TVC) (Day 0) were approximately 6 log CFU/g (Fig. 6a). The relatively high initial TVC likely

reflects the use of minimally processed fresh buffalo milk and artisanal cheese-making conditions. In PLA and PLA/PRP packages, TVC increased significantly ($p < 0.05$) from day 5 to 15, indicating exponential microbial growth. The highest bacterial load ($p < 0.05$) was recorded in PLA films by day 15, suggesting minimal protection from microbial growth.

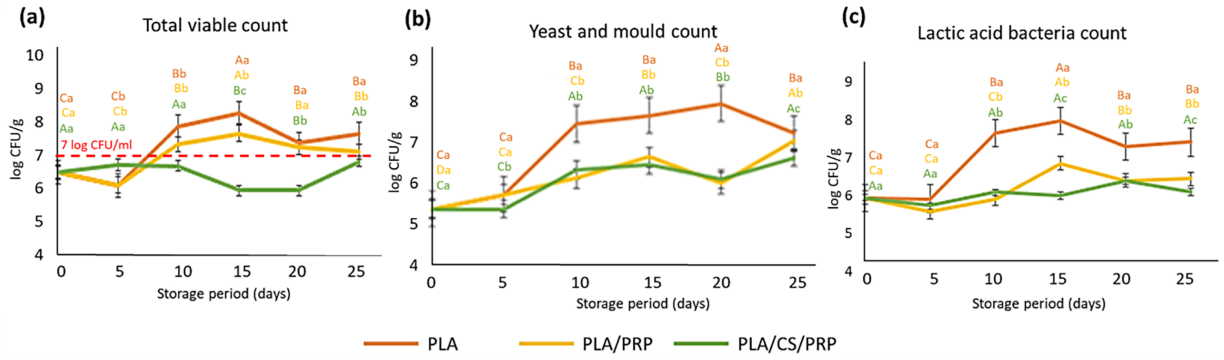

Figure 6: Changes in microbial populations of mozzarella cheese during 25 days of storage at 4°C: (**a**) total viable count, (**b**) yeast and mould count, and (**c**) lactic acid bacteria count in samples packaged with polylactic acid (PLA), polylactic acid/propolis (PLA/PRP), and polylactic acid/chitosan/propolis (PLA/CS/PRP) films. Values are presented as mean ± SD (n = 3). Different lowercase letters indicate significant differences among packaging treatments at the same storage day ($p < 0.05$) while different uppercase letters indicate significant differences among storage days for the same packaging treatment.

In contrast, PLA/CS/PRP maintained a relatively stable TVC ($p \geq 0.05$) up to day 10, indicating an extended lag phase and effective microbial inhibition [83,84]. The delayed microbial growth observed after day 20 may also suggest a prolonged release behaviour of PRP-derived compounds from the CS layer, corroborating the results of pH. The TVC in PLA/CS/PRP was 1.1 log and 0.6 log lower than in PLA and PLA/PRP, respectively, and statistically similar to day 0 ($p \geq 0.05$), evidencing durable antimicrobial efficacy. Based on reported microbiological limit for fresh cheeses at approximately 7 log CFU/g for total mesophilic counts [30,85], the PLA/CS/PRP system maintained microbiological quality for up to 25 days of refrigerated storage, whereas PLA/PRP and neat PLA exceeded acceptable limits at earlier storage intervals. As reported by previous studies, the antibacterial activity of PRP likely stems from the presence of high phenolic content and flavonoids, such as pinocembrin, caffeic acid, and p-coumaric acid [43,86,87]. These compounds disrupt microbial cell membranes by increasing permeability, inducing leakage of intracellular constituents, and interfering with membrane-bound enzymatic systems and energy metabolism [19]. In addition, they can inhibit key biosynthetic pathways, suppressing cell division and delaying microbial growth [88]. However, specific mechanistic pathways were not directly investigated in the present work and should be interpreted as literature-based explanations rather than experimentally confirmed mechanisms.

Yeast and mould growth (Fig. 6b) followed a similar trend, with significantly higher counts observed in neat PLA films. The reduced fungal growth in PRP-containing films confirms its antifungal activity, while further reductions in PLA/CS/PRP systems suggest a potential synergistic effect with CS [45,89]. However, the delayed antifungal effect of CS may be attributed to its internal positioning within the multilayer structure, limiting immediate surface interaction.

Besides contributing to flavour and texture, lactic acid bacteria (LAB) also produce inhibitory compounds such as organic acids, bacteriocins, and hydrogen peroxide [90,91]. LAB populations increased over the storage period (Fig. 6c), with the highest growth ($p < 0.05$) observed in neat PLA films, indicating minimal microbial inhibition. While PRP has been reported to inhibit pathogenic and spoilage-associated

microorganisms at lower concentrations than those required to inhibit potentially probiotic LAB strains [92], the reduction in LAB in PRP- and CS-containing films indicates broader antimicrobial activity, though not complete inhibition. This suggests that the multilayer system enables modulation rather than elimination of microbial populations, which may be advantageous for maintaining product characteristics during storage. However, direct antimicrobial characterisation of the films, such as inhibition zone assays was not performed in the present work. Therefore, the antimicrobial performance of the multilayer films was inferred indirectly from microbial changes observed during refrigerated cheese storage.

4 Conclusion

This study demonstrates the potential application of sequentially coated PLA/CS/PRP multilayer films for preserving fresh mozzarella cheese through improvements in selected physicochemical and microbiological quality attributes during refrigerated storage. The incorporation of PRP introduced significant ($p < 0.05$) changes in optical behaviour, increasing opacity and imparting a characteristic yellow hue, while the addition of the CS layer further reduced transparency without significantly altering colour attributes. These changes reflect the influence of layer composition and interfacial heterogeneity on light transmission within the multilayer structure. Moisture-related properties were strongly governed by the contrasting polarity of the constituent layers. Although the combined incorporation of PRP extract and CS resulted in higher water vapour permeability, likely due to the hydrophilic nature of CS, this effect was partially mitigated during storage, potentially through polymer swelling. Mechanical analysis revealed significant decreases ($p < 0.05$) in tensile strength and elongation at break, suggesting interfacial incompatibility or excessive crosslinking within the CS network. These findings indicate that optimisation of CS crosslinking density and interlayer adhesion will be essential to improve mechanical robustness while preserving functional performance. However, the observed reductions in tensile strength and elongation at break indicate a functional trade-off that may limit certain industrial packaging applications, suggesting that these films are more suitable for applications where antimicrobial functionalities are prioritised over high mechanical load resistance. From a preservation standpoint, PLA/CS/PRP films exhibited the most effective performance for fresh mozzarella cheese, maintaining pH stability and reducing weight loss while significantly ($p < 0.05$) suppressing microbial growth, including total viable counts, yeast, and mould, over 25 days of refrigerated storage. The PLA/CS/PRP films also exhibited relatively low water solubility, contributing to structural stability under refrigerated conditions where condensation-induced moisture exposure is common. Despite the moderate increase in water vapour permeability, the multilayer system provided antimicrobial functionality, making it suitable for high-moisture refrigerated food products in which microbial stability is a more critical quality parameter than strict moisture exclusion. Overall, this work highlights the potential of multilayer design approaches in developing renewable polymer materials with enhanced functional properties. The combination of a bio-based PLA film with naturally derived functional coatings such as CS and PRP offers a promising pathway towards sustainable packaging systems. Residual glutaraldehyde migration was not evaluated in the present study and should be considered a limitation, as potential migration behaviour may influence the food-contact safety and regulatory applicability of the developed multilayer films. Future studies should include advanced characterisation of interfacial interactions, quantitative measurements of coating thickness and coating uniformity, cross-sectional morphological analysis, migration and toxicological assessments, and release kinetics to establish structure-property relationships and confirm the suitability of the multilayer system for food-packaging applications. In addition, sensory evaluation should be conducted in future studies, as the characteristic aroma and flavour of PRP may influence consumer acceptance of packaged dairy products.

Acknowledgement: The authors would like to thank the Faculty of Food Science and Technology, Universiti Putra Malaysia for the permission to use the laboratory and all of the science officers for their kind assistance. During the preparation of this manuscript, the authors utilized OpenAI (GPT-5.5) for linguistic editing such as such as grammar correction and spelling checks. The authors have carefully reviewed and revised the output and accept full responsibility for all content.

Funding Statement: The authors received no specific funding for this study.

Author Contributions: The authors confirm contribution to the paper as follows: study conception and design: Nur Hanani Z. A.; data collection: Ahmad Bustaman N. A. H., Stefan Schiessl; analysis and interpretation of results: Ahmad Bustaman N. A. H., Han Lyn Foong; draft manuscript preparation: Ahmad Bustaman N. A. H., Han Lyn Foong. All authors reviewed and approved the final version of the manuscript.

Availability of Data and Materials: Data available on request from the authors.

Ethics Approval: Not applicable.

Conflicts of Interest: The authors declare no conflicts of interest.

Supplementary Materials: The supplementary material is available online at https://www.techscience.com/doi/10.32604/jrm.2026.02026-0043/s1.

Nomenclature

PLA	Polylactic acid
PBAT	Polybutylene adipate terephthalate
PRP	Propolis
CS	Chitosan
WVP	Water vapour permeability
FTIR	Fourier transform infrared

References

1. Plastics Europe. Plastics—the fast facts 2024 [Internet]. 2024 [cited 2025 Jul 10]. Available from: https://plasticseurope.org/knowledge-hub/plastics-the-fast-facts-2024/.
2. Plastics Europe. Plastics—the fast facts 2023 [Internet]. 2023 [cited 2024 Feb 2]. Available from: https://plasticseurope.org/knowledge-hub/plastics-the-fast-facts-2023/.
3. Pesaranhajiabbas E, Misra M, Mohanty AK. Recent progress on biodegradable polylactic acid based blends and their biocomposites: a comprehensive review. Int J Biol Macromol. 2023;253(4):126231. doi:10.1016/j.ijbiomac.2023.126231.
4. Chuakhao S, Rodríguez JT, Lapnonkawow S, Kannan G, Müller AJ, Suttiruengwong S. Formulating PBS/PLA/PBAT blends for biodegradable, compostable packaging: the crucial roles of PBS content and reactive extrusion. Polym Test. 2024;132(18):108383. doi:10.1016/j.polymertesting.2024.108383.
5. Chen X, Bao J, Shen C, Zhang B, Xu Y, Shen Z. Polymer matrix materials. In: Composite materials engineering, Volume 1: fundamentals of composite materials. Berlin/Heidelberg, Germany: Springer; 2018. p. 151–352. doi:10.1007/978-981-10-5696-3_3.
6. Li YX, Erhunmwunsee F, Liu M, Yang K, Zheng W, Tian J. Antimicrobial mechanisms of spice essential oils and application in food industry. Food Chem. 2022;382(1):132312. doi:10.1016/j.foodchem.2022.132312.
7. Lucas-González R, Yilmaz B, Mousavi Khaneghah A, Hano C, Ali Shariati M, Bangar SP, et al. Cinnamon: an antimicrobial ingredient for active packaging. Food Packag Shelf Life. 2023;35(4):101026. doi:10.1016/j.fpsl.2023.101026.

8. Nirmal NP, Chunhavacharatorn P, Chandra Khanashyam A, Li L, Al-Asmari F. Cinnamon bark oil in water nanoemulsion formulation, characterization, and antimicrobial activities. LWT. 2023;179(4):114671. doi:10.1016/j.lwt.2023.114671.
9. Bodana V, Swer TL, Kumar N, Singh A, Samtiya M, Sari TP, et al. Development and characterization of pomegranate peel extract-functionalized jackfruit seed starch-based edible films and coatings for prolonging the shelf life of white grapes. Int J Biol Macromol. 2024;254:127234. doi:10.1016/j.ijbiomac.2023.127234.
10. Saeed M, Azam M, Ahmad T, Akhtar S, Hussain M, Nasir S, et al. Utilization of pomegranate peel extract as antifungal coating agent against *Fusarium oxysporum* on tomatoes. Food Process Preserv. 2022;46(12):e17157. doi:10.1111/jfpp.17157.
11. Han Lyn F, Nor Adilah A, Gun Hean C, Nur Hanani ZA. Effect of pressure on the supercritical solvent impregnation of pomegranate peel extract into low-density polyethylene films. J Food Eng. 2023;357:111646. doi:10.1016/j.jfoodeng.2023.111646.
12. Sirelkhatim A, Mahmud S, Seeni A, Kaus NHM, Ann LC, Bakhori SKM, et al. Review on zinc oxide nanoparticles: antibacterial activity and toxicity mechanism. Nano Micro Lett. 2015;7(3):219–42. doi:10.1007/s40820-015-0040-x.
13. Liu J, Liu C, Zheng X, Chen M, Tang K. Soluble soybean polysaccharide/nano zinc oxide antimicrobial nanocomposite films reinforced with microfibrillated cellulose. Int J Biol Macromol. 2020;159(90):793–803. doi:10.1016/j.ijbiomac.2020.05.084.
14. Zehetmeyer G, Meira SMM, Scheibel JM, de Oliveira RVB, Brandelli A, Soares RMD. Influence of melt processing on biodegradable nisin-PBAT films intended for active food packaging applications. J Appl Polym Sci. 2016;133(13):43212. doi:10.1002/app.43212.
15. Deng L, Xu R, Zhang S, Lu J, Wang H, Zhou J, et al. Calcium alginate-encapsulated *Propolis* microcapsules: optimization, characterization, and preservation effects on postharvest sweet cherry. Int J Biol Macromol. 2024;282(2):137473. doi:10.1016/j.ijbiomac.2024.137473.
16. Dos Santos Alves MJ, de Sousa MHO, de Moura NF, Cesca K, Verruck S, Monteiro AR, et al. Starch nanoparticles containing phenolic compounds from green propolis: characterization and evaluation of antioxidant, antimicrobial and digestibility properties. Int J Biol Macromol. 2024;255(10):128079. doi:10.1016/j.ijbiomac.2023.128079.
17. Ardjoum N, Chibani N, Shankar S, Fadhel YB, Djidjelli H, Lacroix M. Development of antimicrobial films based on poly(lactic acid) incorporated with *Thymus vulgaris* essential oil and ethanolic extract of Mediterranean propolis. Int J Biol Macromol. 2021;185:535–42. doi:10.1016/j.ijbiomac.2021.06.194.
18. Karpuz E, Palabiyik I. Which method is better for preserving meat and cheese: spraying propolis on the packaging material or directly onto the food? SSRN. 2022. doi:10.2139/ssrn.4244464.
19. Przybyłek I, Karpiński TM. Antibacterial properties of propolis. Molecules. 2019;24(11):2047. doi:10.3390/molecules24112047.
20. Bouchelaghem S. Propolis characterization and antimicrobial activities against *Staphylococcus aureus* and *Candida albicans*: a review. Saudi J Biol Sci. 2022;29(4):1936–46. doi:10.1016/j.sjbs.2021.11.063.
21. Segueni N, Boutaghane N, Asma ST, Tas N, Acaroz U, Arslan-Acaroz D, et al. Review on propolis applications in food preservation and active packaging. Plants. 2023;12(8):1654. doi:10.3390/plants12081654.
22. Garavand F, Rouhi M, Jafarzadeh S, Khodaei D, Cacciotti I, Zargar M, et al. Tuning the physicochemical, structural, and antimicrobial attributes of whey-based poly (L-lactic acid) (PLLA) films by chitosan nanoparticles. Front Nutr. 2022;9:880520. doi:10.3389/fnut.2022.880520.
23. Khodaman E, Barzegar H, Jokar A, Jooyandeh H. Production and evaluation of Physicochemical, Mechanical and Antimicrobial Properties of Chia (*Salvia hispanica* L.) mucilage-gelatin based edible films incorporated with chitosan nanoparticles. J Food Meas Charact. 2022;16(5):3547–56. doi:10.1007/s11694-022-01470-7.
24. Basumatary IB, Mukherjee A, Katiyar V, Dutta J, Kumar S. Chitosan-based active coating for pineapple preservation: evaluation of antimicrobial efficacy and shelf-life extension. LWT. 2022;168(11):113940. doi:10.1016/j.lwt.2022.113940.

25. Jonaidi Jafari N, Kargozari M, Ranjbar R, Rostami H, Hamedi H. The effect of chitosan coating incorporated with ethanolic extract of propolis on the quality of refrigerated chicken fillet. J Food Process Preserv. 2018;42(1):e13336. doi:10.1111/jfpp.13336.
26. Balasubramaniam AK, Elangovan A, Rahman MA, Nayak S, Swain D, Babu HP, et al. Propolis: a comprehensive review on the nature's polyphenolic wonder. Fitoterapia. 2025;183(4):106526. doi:10.1016/j.fitote.2025.106526.
27. Heras M, Huang CC, Chang CW, Lu KH. Trends in chitosan-based films and coatings: a systematic review of the incorporated biopreservatives, biological properties, and nanotechnology applications in meat preservation. Food Packag Shelf Life. 2024;42(3):101259. doi:10.1016/j.fpsl.2024.101259.
28. Faccia M, Gambacorta G, Pasqualone A, Summo C, Caponio F. Quality characteristics and consumer acceptance of high-moisture mozzarella obtained from heat-treated goat milk. Foods. 2021;10(4):833. doi:10.3390/foods10040833.
29. Marrella M, Bertani G, Ricci A, Volpe R, Roustel S, Ferriani F, et al. *Pseudomonas fluorescens* and *Escherichia coli* in fresh mozzarella cheese: effect of cellobiose oxidase on microbiological stability during refrigerated shelf life. Foods. 2022;12(1):145. doi:10.3390/foods12010145.
30. Huang X, Kamgang Nzekoue F, Renzi S, Alesi A, Magdalena Coman M, Pucciarelli S, et al. Influence of modified governing liquid on shelf-life parameters of high-moisture mozzarella cheese. Food Res Int. 2022;159(3):111627. doi:10.1016/j.foodres.2022.111627.
31. Shavisi N, Khanjari A, Basti AA, Misaghi A, Shahbazi Y. Effect of PLA films containing propolis ethanolic extract, cellulose nanoparticle and *Ziziphora clinopodioides* essential oil on chemical, microbial and sensory properties of minced beef. Meat Sci. 2017;124(3):95–104. doi:10.1016/j.meatsci.2016.10.015.
32. Siripatrawan U, Vitchayakitti W. Improving functional properties of chitosan films as active food packaging by incorporating with propolis. Food Hydrocoll. 2016;61(1):695–702. doi:10.1016/j.foodhyd.2016.06.001.
33. Costa SS, Druzian JI, Machado BA, de Souza CO, Guimarães AG. Bi-functional biobased packing of the cassava starch, glycerol, licuri nanocellulose and red propolis. PLoS One. 2014;9(11):e112554. doi:10.1371/journal.pone.0112554.
34. Vargas Romero E, Lim LT, Suárez Mahecha H, Bohrer BM. The effect of electrospun polycaprolactone nonwovens containing chitosan and propolis extracts on fresh pork packaged in linear low-density polyethylene films. Foods. 2021;10(5):1110. doi:10.3390/foods10051110.
35. ASTM D882-02. Standard test method for tensile properties of thin plastic sheeting. Philadelphia, PA, USA: ASTM International; 2002.
36. Ordoñez R, Atarés L, Chiralt A. Multilayer antimicrobial films based on starch and PLA with superficially incorporated ferulic or cinnamic acids for active food packaging purposes. Food Chem Adv. 2023;2(C):100250. doi:10.1016/j.focha.2023.100250.
37. Suriyatem R, Auras RA, Rachtanapun C, Rachtanapun P. Biodegradable rice starch/carboxymethyl chitosan films with added propolis extract for potential use as active food packaging. Polymers. 2018;10(9):954. doi:10.3390/polym10090954.
38. ASTM D644-99. Standard test methods for moisture content of paper and paperboard by oven drying. Philadelphia, PA, USA: ASTM International; 2002.
39. ASTM E96-95. Standard test methods for water vapor transmission of materials. Philadelphia, PA, USA: ASTM International; 1995.
40. Roy S, Priyadarshi R, Rhim JW. Development of multifunctional pullulan/chitosan-based composite films reinforced with ZnO nanoparticles and propolis for meat packaging applications. Foods. 2021;10(11):2789. doi:10.3390/foods10112789.
41. Pastor C, Sánchez-González L, Cháfer M, Chiralt A, González-Martínez C. Physical and antifungal properties of hydroxypropylmethylcellulose based films containing propolis as affected by moisture content. Carbohydr Polym. 2010;82(4):1174–83. doi:10.1016/j.carbpol.2010.06.051.
42. Pérez-Vergara LD, Cifuentes MT, Franco AP, Pérez-Cervera CE, Andrade-Pizarro RD. Development and characterization of edible films based on native cassava starch, beeswax, and propolis. NFS J. 2020;21(3):39–49. doi:10.1016/j.nfs.2020.09.002.

43. Ibrahim MEE, Alqurashi RM. Anti-fungal and antioxidant properties of propolis (bee glue) extracts. Int J Food Microbiol. 2022;361:109463. doi:10.1016/j.ijfoodmicro.2021.109463.
44. Gniewosz M, Pobiega K, Kraśniewska K, Synowiec A, Chaberek M, Galus S. Characterization and antifungal activity of pullulan edible films enriched with propolis extract for active packaging. Foods. 2022;11(15):2319. doi:10.3390/foods11152319.
45. Abarca RL, Vargas F, Medina J, Paredes JC, López BC, Ortiz PA, et al. Development and characterization of films with propolis to inhibit mold contamination in the dairy industry. Foods. 2023;12(8):1633. doi:10.3390/foods12081633.
46. Ahmad Tarmizi AS, Othman MBH, Abdullah Sani MS, Rafiae NN, Rostan NR, Mohamad Ibrahim MN. Conventional blending chitosan lignin nanocomposites hydrogel (CsLNPs) for food coating application. Halalsphere. 2025;5(1):15–23. doi:10.31436/hs.v5i1.119.
47. Kramar A, Rodríguez Ortega I, González-Gaitano G, González-Benito J. Solution casting of cellulose acetate films: influence of surface substrate and humidity on wettability, morphology and optical properties. Cellulose. 2023;30(4):2037–52. doi:10.1007/s10570-022-05026-2.
48. Gupta S, John A, Kumar VSK. Studies on effect of coat thickness on the moisture uptake by a hardwood substrate. Maderas Cienc Tecnol. 2016;18(3):443–56. doi:10.4067/S0718-221X2016005000040.
49. Vogt BD, Soles CL, Lee HJ, Lin EK, Wu WL. Moisture absorption into ultrathin hydrophilic polymer films on different substrate surfaces. Polymer. 2005;46(5):1635–42. doi:10.1016/j.polymer.2004.11.114.
50. Ghannam HE, Talab AS, Dolgano NV, Husse AMS, Abdelmagui NM. Characterization of chitosan extracted from different crustacean shell wastes. J Appl Sci. 2016;16(10):454–61. doi:10.3923/jas.2016.454.461.
51. Milovanovic S, Lukic I, Krgovic N, Tadic V, Radovanovic Z, Tyśkiewicz K, et al. Selection of processing parameters for the integrated supercritical CO_2 extraction from green tea leaves and extract impregnation onto starch-chitosan based films. J Supercrit Fluids. 2024;206(1):106163. doi:10.1016/j.supflu.2023.106163.
52. Li B, Qiu L, Zhang J, Liu S, Xu M, Wang J, et al. Solubilization of chitosan in biologically relevant solvents by a low-temperature solvent-exchange method for developing biocompatible chitosan materials. Int J Biol Macromol. 2024;254(Pt 3):127950. doi:10.1016/j.ijbiomac.2023.127950.
53. Monteil J, Hadj-Sassi A, Dargelos É, Guzman-Barrera N, Poque E, Leal-Calderon F. Method to prepare aqueous propolis dispersions based on phase separation. Food Chem. 2022;389(2):133072. doi:10.1016/j.foodchem.2022.133072.
54. Correa-Pacheco ZN, Bautista-Baños S, de Lorena Ramos-García M, del Carmen Martínez-González M, Hernández-Romano J. Physicochemical characterization and antimicrobial activity of edible propolis-chitosan nanoparticle films. Prog Org Coat. 2019;137(6):105326. doi:10.1016/j.porgcoat.2019.105326.
55. Liu H, Zhao Z, Xu W, Cheng M, Chen Y, Xun M, et al. Preparation, characterization, release and antibacterial properties of cinnamon essential oil microcapsules. Coatings. 2023;13(6):973. doi:10.3390/coatings13060973.
56. YousefniaPasha H, Mohtasebi SS, Tabatabaeekoloor R, Taherimehr M, Javadi A, Soltani Firouz M. Preparation and characterization of the plasticized polylactic acid films produced by the solvent-casting method for food packaging applications. J Food Process Preserv. 2021;45(12):e16089. doi:10.1111/jfpp.16089.
57. Olewnik-Kruszkowska E, Gierszewska M, Wrona M, Nerin C, Grabska-Zielińska S. Polylactide-based films with the addition of poly(ethylene glycol) and extract of propolis-physico-chemical and storage properties. Foods. 2022;11(10):1488. doi:10.3390/foods11101488.
58. Naser AZ, Deiab I, Darras BM. Poly(lactic acid) (PLA) and polyhydroxyalkanoates (PHAs), green alternatives to petroleum-based plastics: a review. RSC Adv. 2021;11(28):17151–96. doi:10.1039/d1ra02390j.
59. Farah S, Anderson DG, Langer R. Physical and mechanical properties of PLA, and their functions in widespread applications—a comprehensive review. Adv Drug Deliv Rev. 2016;107(A):367–92. doi:10.1016/j.addr.2016.06.012.
60. Kamaludin NHI, Ismail H, Rusli A, Sam ST, Gunny AAN. Processing, tensile and morphological characteristics of polylactic acid/chitosan biocomposites prepared by melt compounding technique. In: Proceedings of the 3rd International Postgraduate Conference on Materials, Minerals & Polymer (MAMIP); 2019 Oct 31–Nov 1; Penang, Malaysia. doi:10.1063/5.0016532.

61. Szlachetka O, Witkowska-Dobrev J, Baryła A, Dohojda M. Low-density polyethylene (LDPE) building films—tensile properties and surface morphology. J Build Eng. 2021;44:103386. doi:10.1016/j.jobe.2021.103386.
62. Ghabeer T, Dweiri R, Al-Khateeb S. Thermal and mechanical characterization of polypropylene/eggshell biocomposites. J Reinf Plast Compos. 2013;32(6):402–9. doi:10.1177/0731684412470015.
63. Pérez E, Famá L, Pardo SG, Abad MJ, Bernal C. Tensile and fracture behaviour of PP/wood flour composites. Compos Part B Eng. 2012;43(7):2795–800. doi:10.1016/j.compositesb.2012.04.041.
64. Torres-Hernández YG, Ortega-Díaz GM, Téllez-Jurado L, Castrejón-Jiménez NS, Altamirano-Torres A, García-Pérez BE, et al. Biological compatibility of a polylactic acid composite reinforced with natural chitosan obtained from shrimp waste. Materials. 2018;11(8):1465. doi:10.3390/ma11081465.
65. Pugar D, Haramina T, Leskovac M, Ćurković L. Preparation and characterization of poly(vinyl-alcohol)/chitosan polymer blend films chemically crosslinked with glutaraldehyde: mechanical and thermal investigations. Molecules. 2024;29(24):5914. doi:10.3390/molecules29245914.
66. Gan PG, Sam ST, Abdullah MF, Omar MF, Tan WK. Water resistance and biodegradation properties of conventionally-heated and microwave-cured cross-linked cellulose nanocrystal/chitosan composite films. Polym Degrad Stab. 2021;188:109563. doi:10.1016/j.polymdegradstab.2021.109563.
67. Khouri J, Penlidis A, Moresoli C. Viscoelastic properties of crosslinked chitosan films. Processes. 2019;7(3):157. doi:10.3390/pr7030157.
68. Chieng B, Ibrahim N, Yunus W, Hussein M. Poly(lactic acid)/poly(ethylene glycol) polymer nanocomposites: effects of graphene nanoplatelets. Polymers. 2014;6(1):93–104. doi:10.3390/polym6010093.
69. Qin Y, Li W, Liu D, Yuan M, Li L. Development of active packaging film made from poly (lactic acid) incorporated essential oil. Prog Org Coat. 2017;103:76–82. doi:10.1016/j.porgcoat.2016.10.017.
70. Foong HL, Sulaiman R, Azman EM, Ashari R, Sarıcaoğlu FT, Langowski HC, et al. Development and characterisation of polylactic acid/cinnamon bark oil films: phenolic migration into various food simulants. Food Packag Shelf Life. 2025;48(4):101455. doi:10.1016/j.fpsl.2025.101455.
71. de Carli C, Aylanc V, Mouffok KM, Santamaria-Echart A, Barreiro F, Tomás A, et al. Production of chitosan-based biodegradable active films using bio-waste enriched with polyphenol propolis extract envisaging food packaging applications. Int J Biol Macromol. 2022;213:486–97. doi:10.1016/j.ijbiomac.2022.05.155.
72. Li X, Wu S, Feng T, Wu S, Xu W, Wang Q, et al. Biodegradable quercetin-incorporated poly(lactic acid)/chitosan functional films: a study of the properties and application in enhancing fish preservation. Foods. 2025;14(16):2771. doi:10.3390/foods14162771.
73. Cvetković D, Somogyi Škoc M, Meštrović E, Meštrović IR. Rapid chromatographic and spectroscopic analysis of extracted raw propolis. Molecules. 2025;30(24):4729. doi:10.3390/molecules30244729.
74. Stanicka K, Dobrucka R, Woźniak M, Sip A, Majka J, Kozak W, et al. The effect of chitosan type on biological and physicochemical properties of films with propolis extract. Polymers. 2021;13(22):3888. doi:10.3390/polym13223888.
75. Zemljič LF, Glaser TK, Plohl O, Anžel I, Šimat V, Čagalj M, et al. Biomass-derived plant extracts in macromolecular chitosan matrices as a green coating for PLA films. J Funct Biomater. 2022;13(4):228. doi:10.3390/jfb13040228.
76. Dalsasso RR, Cesca K, Valencia GA, Monteiro AR, Zhang ZJ, Fryer PJ. Active films produced using ginger oleoresin nanoemulsion: characterization and application on mozzarella cheese. Food Hydrocoll. 2025;167(7):111394. doi:10.1016/j.foodhyd.2025.111394.
77. Hong CM, Wendorff WL, Bradley RL Jr. Effects of packaging and lighting on pink discoloration and lipid oxidation of annatto-colored cheeses. J Dairy Sci. 1995;78(9):1896–902. doi:10.3168/jds.s0022-0302(95)76814-x.
78. Kristensen D, Orlien V, Mortensen G, Brockhoff P, Skibsted LH. Light-induced oxidation in sliced Havarti cheese packaged in modified atmosphere. Int Dairy J. 2000;10(1–2):95–103. doi:10.1016/s0958-6946(00)00028-5.
79. Correia Gonçalves M, Cardarelli HR. Mozzarella cheese stretching: a review. Food Technol Biotechnol. 2021;59(1):82–91. doi:10.17113/ftb.59.01.21.6707.
80. Upreti P, Metzger LE. Influence of calcium and phosphorus, lactose, and salt-to-moisture ratio on cheddar cheese quality: pH changes during ripening. J Dairy Sci. 2007;90(1):1–12. doi:10.3168/JDS.S0022-0302(07)72603-6.
81. Jafernik K, Ładniak A, Blicharska E, Czarnek K, Ekiert H, Wiącek AE, et al. Chitosan-based nanoparticles as effective drug delivery systems-a review. Molecules. 2023;28(4):1963. doi:10.3390/molecules28041963.

82. de Moura MR, Aouada FA, Avena-Bustillos RJ, McHugh TH, Krochta JM, Mattoso LHC. Improved barrier and mechanical properties of novel hydroxypropyl methylcellulose edible films with chitosan/tripolyphosphate nanoparticles. J Food Eng. 2009;92(4):448–53. doi:10.1016/j.jfoodeng.2008.12.015.
83. Motelica L, Ficai D, Oprea OC, Ficai A, Andronescu E. Smart food packaging designed by nanotechnological and drug delivery approaches. Coatings. 2020;10(9):806. doi:10.3390/coatings10090806.
84. Chang S, Mohammadi Nafchi A, Baghaie H. Development of an active packaging based on polyethylene containing linalool or thymol for mozzarella cheese. Food Sci Nutr. 2021;9(7):3732–9. doi:10.1002/fsn3.2334.
85. Sharafi H, Moradi M, Amiri S. Application of cheese whey containing postbiotics of *Lactobacillus acidophilus* LA5 and *Bifidobacterium animalis* BB12 as a preserving liquid in high-moisture mozzarella. Foods. 2022;11(21):3387. doi:10.3390/foods11213387.
86. Cottica SM, Sawaya ACHF, Eberlin MN, Franco SL, Zeoula LM, Visentainer JV. Antioxidant activity and composition of propolis obtained by different methods of extraction. J Braz Chem Soc. 2011;22(5):929–35. doi:10.1590/s0103-50532011000500016.
87. Ezazi A, Javadi A, Jafarizadeh-Malmiri H, Mirzaei H. Development of a chitosan-propolis extract edible coating formulation based on physico-chemical attributes of hens' eggs: optimization and characteristics edible coating of egg using chitosan and propolis. Food Biosci. 2021;40(2):100894. doi:10.1016/j.fbio.2021.100894.
88. Grinn-Gofroń A, Kołodziejczak M, Hrynkiewicz R, Lewandowski F, Bębnowska D, Adamski C, et al. Antimicrobial potential of bee-derived products: insights into honey, propolis and bee venom. Pathogens. 2025;14(8):780. doi:10.3390/pathogens14080780.
89. Aparicio-García PF, Ventura-Aguilar RI, Del Río-García JC, Hernández-López M, Guillén-Sánchez D, Salazar-Piña DA, et al. Edible chitosan/propolis coatings and their effect on ripening, development of *Aspergillus flavus*, and sensory quality in fig fruit, during controlled storage. Plants. 2021;10(1):112. doi:10.3390/plants10010112.
90. Ibrahim SA, Ayivi RD, Zimmerman T, Siddiqui SA, Altemimi AB, Fidan H, et al. Lactic acid bacteria as antimicrobial agents: food safety and microbial food spoilage prevention. Foods. 2021;10(12):3131. doi:10.3390/foods10123131.
91. Punia Bangar S, Suri S, Trif M, Ozogul F. Organic acids production from lactic acid bacteria: a preservation approach. Food Biosci. 2022;46(10):101615. doi:10.1016/j.fbio.2022.101615.
92. Ferreira de Brito L, Bergara Pereira F, Lorenzon MC, Castro RN, Laureano Melo R, Guerra AF, et al. What is the effect of propolis extracts against pathogenic microorganisms and on potentially probiotic strains of *Lacticaseibacillus* and *Limosilactobacillus*? ACS Food Sci Technol. 2022;2(3):493–502. doi:10.1021/acsfoodscitech.1c00267.